

Preparation of Highly Transparent 13F-Modified Nano-Silica/Polymer Hydrophobic Hard Coatings on Plastic Substrates

Chao-Ching Chang^{1,2}, Zi-Min Lin¹, Shu-Hui Huang¹ and Liao-Ping Cheng^{1,2*}

¹Department of Chemical and Materials Engineering, Tamkang University, Tamsui, Taiwan 251, R.O.C.

²Energy and Opto-Electronic Materials Research Center, Tamkang University, Tamsui, Taiwan 251, R.O.C.

Abstract

Silica nanoparticles synthesized from tetraethoxysilane (TEOS) via a sol–gel process were surface-modified by using 3-(trimethoxysilyl)propyl methacrylate (MSMA) and 1H, 1H, 2H, 2H-perfluorooctyltriethoxysilane (13F). MSMA acted as a coupling agent and a C=C provider, whereas 13F was employed to enhance hydrophobicity. The surface-modified silica particles together with a multi-functional monomer were UV-cured to yield highly transparent thin films (~7 μm) on plastic substrates. Both FE-SEM imaging and UV–visible spectroscopy confirmed uniform dispersion of nano-silica in the hybrid thin films. The coating surfaces were extremely smooth, with average roughness over the range 1.0–2.3 nm based on profilometric measurements. X-ray photoelectron spectroscopy indicated that surface-modified silica particles have migrated to the top surface to reduce the surface energy. Therefore, only a small dosage of 1 mol% (vs. TEOS) was enough to engender surface hydrophobicity with water contact angle of 100°. Furthermore, all of the prepared coatings were hard with pencil hardness reached 6H, and they adhered strongly to the poly(methyl methacrylate) substrate according to the peel test.

Key Words: Colloidal Silica, Hard Coating, UV-curing, Plastic Substrate, Hydrophobic

1. Introduction

Materials with a low surface energy are naturally hydrophobic. When applied as a thin film on a substrate, they create a surface that is water-repelling, easy-to-clean, and anti-smudging. This remarkable property is currently employed in a wide variety of industries. For example, a hydrophobic surface can be used to protect electronic devices from corrosion due to its water-repelling character. Fluoro-compounds with a low surface energy were frequently utilized to prepare transparent hydrophobic and super-hydrophobic coatings. Many useful synthetic and/or processing strategies have been developed

over the past decade. In spite of the extremely high contact angle being attained, the micro/nano structures on the outmost surface are very delicate and prone to damaging by mechanical contact, e.g., during cleaning, which may cause the surface to lose hydrophobicity. If the coating is to be applied on a plastic substrate, the high temperature post-formation treatments commonly used to achieve adherence and to impart hydrophobicity become more difficult. Furthermore, to serve as an optical coating, such as on lenses, mobile phones, touch panels, waveguides etc., it is also desirable to have high transparency over a wide wavelength range. Hence transparent hydrophobic or super-hydrophobic thin films prepared on plastic substrates have attracted attention in recent years [1–11].

*Corresponding author. E-mail: lpcheng@mail.tku.edu.tw

On the other hand, transparent hard coatings are frequently applied on plastic surfaces as protective layers against mechanical damages, and suited to optical applications such as lenses, mobile phones, touch panels, waveguides [12–20]. In addition to protective purpose, hard coatings may be functionalized to impart specific properties, such as hydrophobicity. In the present research, preparation of highly transparent hard coatings that exhibit easy-to-clean (contact angle $> 90^\circ$) character on plastic substrates was our major concern. Formulations based on inorganic-organic nanocomposites were employed, for which the inorganic part consisted of silica nanoparticles that were surface-modified both by using 3-(trimethoxysilyl)propyl methacrylate and 1H, 1H, 2H, 2H-perfluorooctyltriethoxysilane, while the organic part was a cross-linked network of the multi-functional acrylic monomer. The role of MSMA was dual: on one hand, it linked covalently to silica particles by means of Si–O–Si bonds, and on the other hand it provided methacrylate groups that allowed co-polymerization with the acrylic monomer during a UV-curing process. In the extreme case, a hydrophobic coating with contact angle of 106° , pencil hardness of 6H, and $\sim 100\%$ transmittance (380–780 nm) can be prepared. Detailed preparation and

analyses of the products are given in below.

2. Experimental

2.1 Materials

Tetraethoxysilane (TEOS, $> 98\%$) was purchased from Fluka. 3-(Trimethoxysilyl)propyl methacrylate (MSMA, 98%) and the hexa-functional crosslinking agent, dipentaerythritol penta-/hexaacrylate (DPHA, reagent grade), were purchased from Aldrich. The fluoroalkylsilane, 1H, 1H, 2H, 2H-perfluorooctyltriethoxysilane (called 13F hereinafter), was purchased from ABCR. 2-Propanol (IPA, 99.5%) purchased from Fluka was used as the solvent for synthesis of surface-modified silica nanoparticles. Hydrochloric acid (37 wt%) was purchased from J. T. Baker. The photo-initiator, 2-hydroxy-2-methyl-1-phenyl-1-propanone (Darocure 1173), was purchased from Ciba-Geigy. All materials were used as received.

2.2 Preparation of Silica Particles

The synthetic procedure of surface-modified silica sol is shown in Figure 1 [10,11,21–24]. TEOS (18.87 g) was mixed with IPA (2.22 g) to form a homogeneous solution. Then, aqueous HCl (pH 1.2) was added under

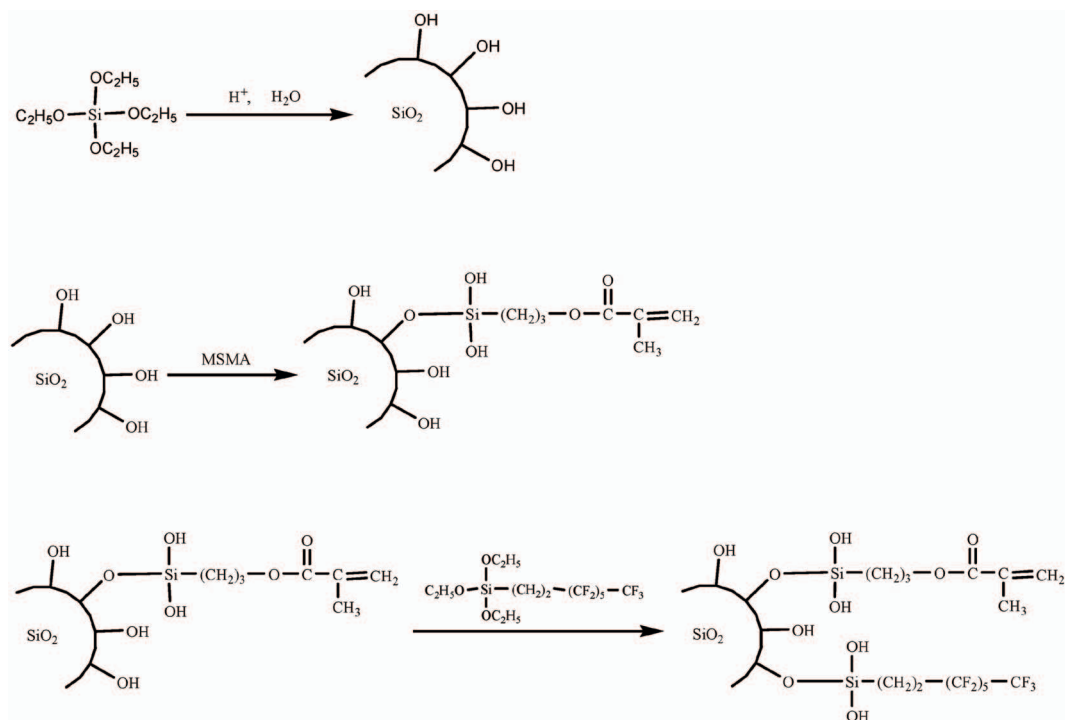


Figure 1. Synthetic route of the silica nanoparticles modified both by 13F and MSMA.

agitation to induce the sol–gel reaction. The molar ratio of $\text{H}_2\text{O}/\text{TEOS}$ was set to 4. The solution was stirred for 3 h at room temperature, after which MSMA (5.0 g, $\text{TEOS}/\text{MSMA} = 4.5$) and additional aqueous HCl (with a molar ratio of $\text{H}_2\text{O}/\text{MSMA} = 3$) were very slowly dropped into the formed silica sol using a syringe pump. The reaction was continued for 3 h and the obtained MSMA-grafted silica was called MSiO_2 . An appropriate amount of 13F (dissolved in aqueous IPA, with the molar ratio of $13\text{F}/\text{H}_2\text{O}/\text{IPA} = 1/2/1$) was added into the MSiO_2 sol under vigorous agitation. The reaction was allowed to proceed for 3 h, and the modified silica was called MFSiO_2 . The added amounts of 13F, expressed in terms of the ratio $R = 13\text{F}/\text{TEOS}$, for the above reaction are listed in Table 1. The theoretical solid contents in the final solutions of the MSiO_2 and MFSiO_2 sols were ~ 25 wt%.

2.3 Preparation of Coatings

To prepare a UV-sensitive coating sol, appropriate amounts of DPHA and photo-initiator, Darocure 1173, were added into the synthesized MFSiO_2 sol under mild agitation. The weight ratio of MFSiO_2 sol/DPHA/1173 was 10/1.67/0.21, and the solid content was found to be 40 wt%. Then, the sol was uniformly spread on a PMMA substrate by doctor-blade coating, pre-baked at 80°C for 30 s on a hot plane, followed by UV irradiation with a conventional medium-pressure mercury lamp (broadband, ~ 960 mJ/cm^2) to yield a cured film. The samples designated as Fx stand for prepared hybrid coatings, where $x = 1, 5, 10, 30,$ and 50 denote the used MFSiO_2 sols with R values = 0.001, 0.005, 0.01, 0.03 and 0.05, respectively.

2.4 Characterization

Infrared absorption spectra of the silica sol were obtained using a Fourier transform infrared spectrophotometer (FTIR, Nicolet iS10, Thermo Scientific). Samples were prepared by dropping appropriate amount of silica sol on a KBr disc, and then the solvent was removed under vacuum. The size and size distribution of silica particles suspended in the sol were determined by dynamic light scattering (DLS), using a Zetasizer (DTS 3000HS, Malvern), at 25°C at the concentration of 1 wt%. Morphology of the cured film was observed using a field emission scanning electron microscope (FE-SEM,

S4800, Hitachi). The samples were vacuum-dried and then fractured in liquid nitrogen to expose the cross section. The light transmittance of the prepared coatings was measured by a UV–visible spectrometer (Evolution 300, Thermo Scientific) over the wavelength range of 200–1000 nm with respect to a PMMA substrate. The average transmittance of the film was calculated from 380 to 780 nm. The thickness and surface average roughness (R_a) of the coatings were examined by a surface profilometer (EZSTEP, Force Precision Instrument Corporation). The static contact angle between water and coating surface was measured by a First Ten Ångströms FTÅ 125 contact angle/surface energy analyzer at room temperature. For each sample, measurement was taken at five different locations and the average value was reported with deviation. The tape test (ASTM D3359), also called peel test, was carried out to evaluate the adhesion strength of the film coated on a PMMA substrate. The degree of adhesion between the film and the substrate was counted as the percentage of the residual film on the substrate after peeling by tapes (3M–610). The hardness of the cured films was examined by the industrial pencil hardness test (ASTM D3363), using pencils of different hardness at the load of 500 g. The compositions of various species on the coating surface were analyzed by the X-ray photoelectron spectroscope (XPS, VG ESCA Scientific Theta Probe). Aluminum K_α radiation (1486.6 eV) was used as the X-ray source with an X-ray spot size of 15–400 μm .

3. Results and Discussion

3.1 Analyses of MFSiO_2 Sols

The FTIR spectrum of the 13F modified silica ($R =$

Table 1. Added amounts of 13F for preparing MFSiO_2 sols

R	MSiO_2 sol (g)	13F (g)	13F/TEOS (mol/mol)	F/Si ^a (at./at.)
0	36.21	0	0	0
0.001	36.21	0.0463	0.001	0.011
0.005	36.21	0.2315	0.005	0.053
0.010	36.21	0.463	0.01	0.106
0.030	36.21	1.3892	0.03	0.312
0.050	36.21	2.3153	0.05	0.511

^a Theoretical value.

0.05), is demonstrated in Figure 2 together with MSiO_2 and 13F. The absorption bands at 1050 and 454 cm^{-1} correspond to the stretching and bending vibrations of Si–O–Si bonds, respectively. The band at 948 cm^{-1} is assigned to the Si–OH groups on the silica particles stemming from hydrolysis of TEOS. The absorptions of C=C and C=O for the MSMA moieties are located at 1620 cm^{-1} and 1710 cm^{-1} , respectively. The broad band around 3422 cm^{-1} stands for the asymmetric stretching of various –OH groups, e.g., from moisture, residual solvent, silica, etc. The signal associated with 13F could only be found at 691 cm^{-1} ; other characteristic peaks of 13F are not in evidence because of overlapping with those of MSMA. Furthermore, it is noted that the C=C on the modified SiO_2 particles are photo-sensitive, which can polymerize with the hexa-functional monomer, DPHA, to form a cross-linked network via a UV-curing process.

The size of particles dispersed in the sol was determined by the dynamic light scattering (DLS) method. The scattering profile of the sample F50 indicated that the particles distributed over a rather small size range of 1.3–13 nm, with the peak maximum located at 7.9 nm. Such distribution is consistent with those reported in the literature for MSiO_2 nanoparticles synthesized via the sol–gel route under strong acid conditions [21,23]. Particle sizes of other sols were also determined, and they fell over the range 4–8 nm and increased slightly with increasing 13F dosage.

3.2 Properties of the Coatings

The widely used pencil test was employed to examine the hardness of the coatings cured on PMMA sub-

strates. The tested results are summarized in Table 2. A high hardness of 7H was established by the coating F0 (cross-linked network of MSiO_2 and DPHA) comparing with 3H for the PMMA substrate, as a result of the strong organic–inorganic network built of the multi-functional DPHA and the nano-silica, MSiO_2 . Incorporation of 13F downgraded slightly the hardness to 6H due to the long alkyl tail of 13F molecule. As to the adhesiveness, all samples showed perfect attachment to the PMMA substrate, irrespective of the 13F content. This suggests that a fine dispersion of nano-silica in the polymer host has been achieved. Otherwise, if phase separation occurred, the large separated inorganic phases may deteriorate the adhesion, as shown in previous publications [25,26].

Figure 3 shows the cross-sectional SEM image of the coating, F10. It is very uniform without any identifiable aggregated phases at a resolvable scale of ca. 30 nm (cf. the high magnification image in the inset), which further confirms good compatibility between polymer and modified silica being achieved. As the coating surface was smooth, its thickness could be measured to be $7\text{ }\mu\text{m}$. The UV–visible spectra of all prepared coatings showed that these coatings were highly transparent. For example, the UV–visible spectrum of the sample F50 is shown in Figure 4. The average transmittances over the visible range (with reference to PMMA substrate) of all prepared coatings are listed in Table 2. The transmittance of the sample F0 is ~99%, while those of the others approach 100%. The surface average roughness (R_a) of various coatings was determined by profilometry, and the results are listed in Table 2. The surfaces are very smooth with an average roughness over the range 0.9–2.3 nm. For

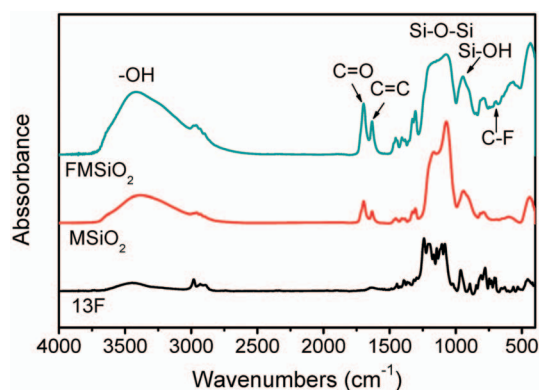


Figure 2. FTIR spectra of 13F, MSiO_2 , and MFSiO_2 ($R = 0.05$).

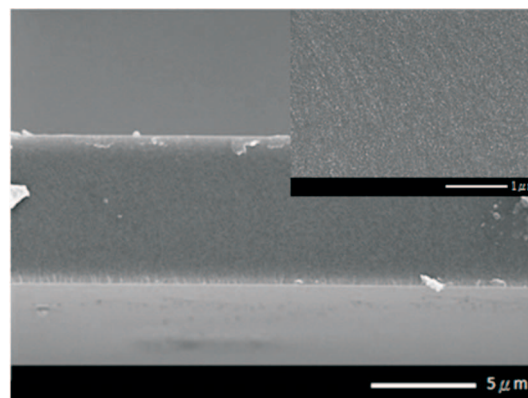


Figure 3. FE-SEM images of the cross-section of the coating, F10.

coatings F0 and F1, the R_a values are somewhat higher than the others with higher fluorine contents. That is, in addition to providing hydrophobicity, 13F could also flatten the surface due to its low surface energy. The coating thickness of F10, as determined by profilometry, was $\sim 7.3 \mu\text{m}$, which was in agreement with the value determined by SEM imaging. As the solid content for all coating sols was kept at 40%, the thicknesses of all coatings was very close, over the range 6.4–8.8 μm , cf. Table 2.

For a smooth surface, the hydrophobicity could be characterized by its water contact angle. If the contact angle is higher than 90° , the surface may be termed easy-to-clean (ETC). Cross-linked DPHA is a polymer of intermediate hydrophobicity with water contact angles near 65° due to its abundance of ester groups in the molecule. To prepare ETC hard coatings based on DPHA, the highly hydrophobic agent, 13F, was incorporated as the nano-silica modifier. The contact angles of various prepared coatings are shown in Table 2. It is interesting to find that by adding just a small amount of 13F, the contact angle could be raised considerably. For example, the contact angle of the sample F10 has reached a high value of 100° , even though merely 1 mol% (versus TEOS) of 13F was added. It is also noted that enhance-

ment of hydrophobicity was most effective for lower 13F-content cases; beyond the dosage level of $R = 0.01$, contact angle of the coatings increased only marginally. Specifically, the sample F50 contained 5 times more 13F than F10; yet its contact angle was only 6 degrees higher than that of F10. Such seemingly peculiar phenomenon could roughly be rationalized by examining the fluorine content data on the vicinity of the top surface, as determined by XPS analyses. In Figure 5, spectra of the coating samples containing different amounts 13F are demonstrated. The Si, C, O, and F peaks were identified with binding energies, 167, 297, 542, and 698 eV, respectively. The amounts (at.%) of F and Si, as well as F/Si for each sample are listed in Table 3. Note that XPS measures the elemental composition from the top 0 to 10 nm of the coating being analyzed. As expected the amount of F on the top surface increased with increasing 13F dosage, but the value was much larger than that calculated from the coating sol for each of the samples. The amount of Si on the top surface also increased with increasing 13F dosage. These results showed that the dispersion of 13F in the coating was not homogenous. 13F spontaneously migrated towards the top surface so as to reduce the surface energy of the coating. However, the

Table 2. Properties of various silica-containing hard coatings

Sample	Hardness	Adhesion (%)	Thickness (μm)	Roughness (nm)	Transmittance (%)	Contact angle (degree)
F0	7H	100		2.13	99.0	72
F1	6H	100	7.1	2.26	99.8	78
F5	6H	100	7.9	1.28	99.8	88
F10	6H	100	7.3	0.94	99.8	100
F30	6H	100	6.4	1.01	99.9	104
F50	6H	100	8.8	0.99	100.0	106

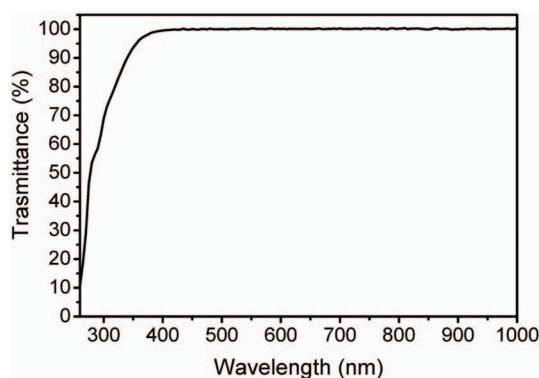


Figure 4. UV-visible spectrum of the coating, F50.

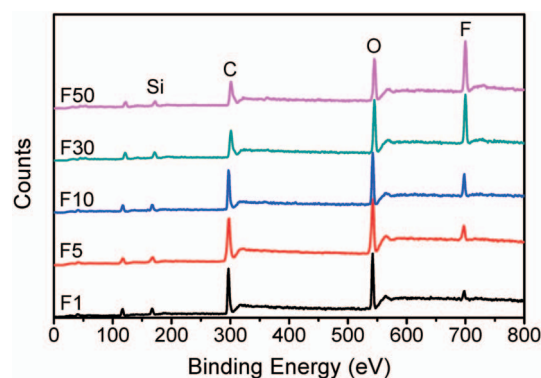


Figure 5. XPS spectra of various 13F-containing coatings.

Table 3. Atomic ratios on the top surfaces of the MFSiO₂-containing coatings

Sample	C (at.%)	O (at.%)	F (at.%)	Si (at.%)	F/Si (at./at.)
F1	67.67	23.66	2.32	6.35	0.365
F5	60.08	26.26	4.65	8.29	0.561
F10	53.95	28.00	9.06	9.00	1.007
F30	42.40	29.15	19.42	9.03	2.151
F50	32.90	30.71	26.80	9.58	2.797

benefit was slow down when the 13F dosage was increased. The reason for the large amount of F on the top surface was resulted from the disproportionately grafted and the un-grafted 13F. For each 13F dosage, the amount of 13F on every silica particle should not be the same and was a distribution with an average value. The particles grafted more 13F migrated towards the top surface more effectively. In addition, the un-grafted 13F also spontaneously migrated towards the top surface. However, the contact angle of the sample of the highest 13F dosage was still limited to a value of 106°. That means excess amount of F on the top surface can't aid the increase in the contact angle of the coating.

4. Conclusions

A new type of highly transparent easy-to-clean hard coatings was developed through the employment of 13F-modified silica particles and DPHA. The UV-cured coatings were very smooth with average roughness over the range 0.9–2.3 nm, and they demonstrated high hardness (6H), transparency (~100%), and water contact angle (~100°). Also, because 13F-modified silica and un-grafted 13F tended to migrate to the top surface, only a small dosing level of 1% (vs TEOS) was enough to generate hydrophobicity.

Acknowledgement

The authors thank the National Science Council of Taiwan for the financial support (NSC 96-2628-E-032-001-MY3).

References

- [1] Schmidt, H., "Nanoparticles by Chemical Synthesis, Processing to Materials and Innovative Applications," *Applied Organometallic Chemistry*, Vol. 15, No. 5, pp. 331–343 (2001). doi: 10.1002/aoc.169
- [2] Daoud, W. A., Xin, J. H. and Tao, X., "Superhydrophobic Silica Nanocomposite Coating by a Low-Temperature Process," *Journal of the American Ceramic Society*, Vol. 87, No. 9, pp. 1782–1784 (2004). doi: 10.1111/j.1551-2916.2004.01782.x
- [3] Dodiuk, H., Rios, P. F., Dotan, A. and Kenig, S., "Hydrophobic and Self-Cleaning Coatings," *Polymers for Advanced Technologies*, Vol. 18, No. 9, pp. 746–750 (2007). doi: 10.1002/pat.957
- [4] Rios, P. F., Dodiuk, H., Kenig, S., McCarthy, S. and Dotan, A., "Durable Ultra-Hydrophobic Surfaces for Self-Cleaning Applications," *Polymers for Advanced Technologies*, Vol. 19, No. 11, pp. 1684–1691 (2008). doi: 10.1002/pat.1208
- [5] Budunoglu, H., Yildirim, A., Guler, M. O. and Bayindir, M., "Highly Transparent, Flexible and Thermally Stable Superhydrophobic ORMOSIL Aerogel Thin Films," *ACS Applied Materials and Interfaces*, Vol. 3, No. 2, pp. 539–545 (2011). doi: 10.1021/am101116b
- [6] Ebert, D. and Bhushan, B., "Transparent, Superhydrophobic and Wear-Resistant Coatings on Glass and Polymer Substrates Using SiO₂, ZnO, and ITO Nanoparticles," *Langmuir*, Vol. 28, No. 31, pp. 11391–11399 (2012). doi: 10.1021/la301479c
- [7] De, S., Jana, D., Medda, S. K. and De, G., "Wavelength Selective Antireflective Coatings on Plastics with Hydrophobic Surfaces," *Industrial and Engineering Chemistry Research*, Vol. 52, No. 23, pp. 7737–7745 (2013). doi: 10.1021/ie400395c
- [8] Boudot, M., Gaud, V., Louarn, M., Selmane, M. and Grosso, D., "Sol-Gel Based Hydrophobic Antireflective Coatings on Organic Substrates: a Detailed Investigation of Ammonia Vapor Treatment (AVT)," *Chemistry of Materials*, Vol. 26, No. 5, pp. 1822–1833 (2014). doi: 10.1021/cm403787v
- [9] Li, H., Jiang, M., Hu, D., Yan, Y., Li, Q., Dong, L. and Xiong, C., "Solvent-Free Zirconia Nanofluids/Silica Single-Layer Multifunctional Hybrid Coatings," *Colloids and Surfaces A: Physicochemical and Engineering Aspects, A*, Vol. 464, No. 5, pp. 26–32 (2015). doi: 10.1016/j.colsurfa.2014.10.014

- [10] Chang, C. C., Oyang, T. Y., Hwang, F. H., Chen, C. C. and Cheng, L. P., "Preparation of Polymer/Silica Hybrid Hard Coatings with Enhanced Hydrophobicity on Plastic Substrates," *Journal of Non-Crystalline Solids*, Vol. 358, No. 1, pp. 72–76 (2012). doi: [10.1016/j.jnoncrysol.2011.08.024](https://doi.org/10.1016/j.jnoncrysol.2011.08.024)
- [11] Chang, C. C., Oyang, T. Y., Chen, Y. C., Hwang, F. H. and Cheng, L. P., "Preparation of Hydrophobic Nanosilica-Filled Polyacrylate Hard Coatings on Plastic Substrates," *Journal of Coatings Technology Research*, Vol. 11, No. 3, pp. 381–386 (2014). doi: [10.1007/s11998-013-9540-0](https://doi.org/10.1007/s11998-013-9540-0)
- [12] Gilberts, J., Tinnemans, A. H. A., Hogerheide, M. P. and Koster, T. P. M., "UV Curable Hard Transparent Hybrid Coating Materials on Polycarbonate Prepared by the Sol–Gel Method," *Journal of Sol–Gel Science and Technology*, Vol. 11, No. 2, pp. 153–159 (1998). doi: [10.1023/A:1008693413965](https://doi.org/10.1023/A:1008693413965)
- [13] Chang, C. C., Wang, S. H., Chen, Y. C. and Cheng, L. P., "Preparation and Characterization of Spiroanthoxazine/polyacrylate Photochromic Hard Coatings on Plastic Substrates," *Journal of Applied Science and Engineering*, Vol. 17, No. 2, pp. 167–174 (2014). doi: [10.6180/jase.2014.17.2.07](https://doi.org/10.6180/jase.2014.17.2.07)
- [14] Chou, T. P. and Cao, G., "Adhesion of Sol-Gel-Derived Organic–Inorganic Hybrid Coatings on Polyester," *Journal of Sol-Gel Science and Technology*, Vol. 27, No. 1, pp. 31–41 (2003). doi: [10.1023/A:1022675809404](https://doi.org/10.1023/A:1022675809404)
- [15] Schottner, G., Rose, K. and Posset, U., "Scratch and Abrasion Resistant Coatings on Plastic Lenses—State of the Art, Current Developments and Perspectives," *Journal of Sol-Gel Science and Technology*, Vol. 27, No. 1, pp. 71–79 (2003). doi: [10.1023/A:1022684011222](https://doi.org/10.1023/A:1022684011222)
- [16] Almaral-Sanchez, J. L., Rubio, E., Mendoza-Galvan, A. and Ramirez-Bon, R., "Red Colored Transparent PMMA–SiO₂ Hybrid Films," *Journal of Physics and Chemistry of Solids*, Vol. 66, No. 10, pp. 1660–1667 (2005). doi: [10.1016/j.jpcs.2005.06.006](https://doi.org/10.1016/j.jpcs.2005.06.006)
- [17] Blanc, D., Last, A., Franc, J., Pavan, S. and Loubet, J. L., "Hard UV-Curable Organo-Mineral Coatings for Optical Applications," *Thin Solid Films*, Vol. 515, No. 3, pp. 942–946 (2006). doi: [10.1016/j.tsf.2006.07.177](https://doi.org/10.1016/j.tsf.2006.07.177)
- [18] Toselli, M., Marini, M., Fabbri, P., Messori, M. and Pilati, F., "Sol–Gel Derived Hybrid Coatings for the Improvement of Scratch Resistance of Polyethylene," *Journal of Sol-Gel Science and Technology*, Vol. 43, No. 1, pp. 73–83 (2007). doi: [10.1007/s10971-007-1560-8](https://doi.org/10.1007/s10971-007-1560-8)
- [19] Jeon, S. J., Lee, J. J., Kim, W., Chang, T. S. and Koo, S. M., "Hard Coating Films Based on Organosilane-Modified Boehmite Nanoparticles under UV/Thermal Dual Curing," *Thin Solid Films*, Vol. 516, No. 12, pp. 3904–3909 (2008). doi: [10.1016/j.tsf.2007.07.165](https://doi.org/10.1016/j.tsf.2007.07.165)
- [20] Wu, L. Y. L., Boon, L., Chen, Z. and Zeng, X. T., "Adhesion Enhancement of Sol–Gel Coating on Polycarbonate by Heated Impregnation Treatment," *Thin Solid Films*, Vol. 517, No. 17, pp. 4850–4856 (2009). doi: [10.1016/j.tsf.2009.03.086](https://doi.org/10.1016/j.tsf.2009.03.086)
- [21] Chen, C. C., Lin, D. J., Don, T. M., Huang, F. H. and Cheng, L. P., "Preparation of Organic–Inorganic Nano-Composites for Antireflection Coatings," *Journal of Non-Crystalline Solids*, Vol. 354, No. 32, pp. 3828–3835 (2008). doi: [10.1016/j.jnoncrysol.2008.04.010](https://doi.org/10.1016/j.jnoncrysol.2008.04.010)
- [22] Lee, C. K., Don, T. M., Lai, W. C., Chen, C. C., Lin, D. J. and Cheng, L. P., "Preparation and Properties of Nano-Silica Modified Negative Acrylate Photoresist," *Thin Solid Films*, Vol. 516, No. 23, pp. 8399–8407 (2008). doi: [10.1016/j.tsf.2008.04.051](https://doi.org/10.1016/j.tsf.2008.04.051)
- [23] Huang, F. H., Chang, C. C., Oyang, T. Y., Chen, C. C. and Cheng, L. P., "Preparation of Almost Dispersant-Free Colloidal Silica with Superb Dispersibility in Organic Solvents and Monomers," *Journal of Nanoparticle Research*, Vol. 13, No. 9, pp. 3885–3897 (2011). doi: [10.1007/s11051-011-0342-y](https://doi.org/10.1007/s11051-011-0342-y)
- [24] Chang, C. C., Huang, F. H., Chang, H. H., Don, T. M., Chen, C. C. and Cheng, L. P., "Preparation of Water-Resistant Antifog Hard Coatings on Plastic Substrate," *Langmuir*, Vol. 28, No. 49, pp. 17193–17201 (2012). doi: [10.1021/la304176k](https://doi.org/10.1021/la304176k)
- [25] Lin, D. J., Chen, C. C., Su, Y. C., Huang, S. H. and Cheng, L. P., "Preparation of Silica Filled Poly(2-hydroxymethyl methacrylate) Nanocomposites Cured by Photoirradiation during the Sol–Gel Process," *Journal of Applied Polymer Science*, Vol. 94, No. 5, pp. 1927–1935 (2004). doi: [10.1002/app.21097](https://doi.org/10.1002/app.21097)

- [26] Lin, D. J., Don, T. M., Chen, C. C., Lin, B. Y., Lee, C. K. and Cheng, L. P., "Preparation of a Nanosilica-Modified Negative-Type Acrylate Photoresist," *Journal of Applied Polymer Science*, Vol. 107, No. 2, pp. 1179–1181 (2008). doi: [10.1002/app.27151](https://doi.org/10.1002/app.27151)

Manuscript Received: Apr. 17, 2015

Accepted: Sep. 12, 2015